Capturing plasmonic behaviors in light scattering by spheres using finite element methods and asymptotic quadrature

Camille Carvalho, Arnold Kim, Benjamin Latham

Capturing plasmonic behaviors in light scattering by spheres using finite element methods and asymptotic quadrature

Camille Carvalho[2,1], **Arnold Kim**[2], **Benjamin Latham**[2,*]

[1]Univ Lyon, INSA Lyon, UJM, UCBL, ECL, CNRS UMR 5208, ICJ, F-69621, France

[2]Department of Applied Mathematics, UC Merced, Merced, United States of America

*Email: blatham@ucmerced.edu

Abstract

We present a Finite Element Method (FEM) based approach to capture plasmonic behaviors in light scattering by metallic spheres. Surface plasmons are highly oscillatory waves localized to the interface between a dielectric (air, vacuum) and a metal (gold, silver). As surface plasmons lead to large field enhancements, they are useful for high-resolution imaging and other applications. It is challenging to capture them numerically, and standard methods do not succeed. In the context of spherical scatterers, we identify where plasmonic excitations can arise, and propose an approach to extract the fast-scale plasmonic behavior from the formulation, allowing FEM to approach the slow (smooth) part of the solution.

Keywords: Finite Element Methods, Surface Plasmons, Resonances, Scattering

1 Problem setting

For simplicity we consider time-harmonic scattering of scalar waves in a homogeneous background medium. The plane wave $u^{\text{in}} = e^{ikz}$ with wavenumber $k > 0$ is incident on the metal sphere corresponding to domain $\Omega = \{|x| < 1\}$ with boundary $\partial\Omega = \{|x| = 1\}$ and closure $\bar{\Omega} = \Omega \cup \partial\Omega$. Let $\varepsilon(x) = 1$, $x \in E := \mathbb{R}^3 \setminus \bar{\Omega}$ and $\varepsilon(x) = \varepsilon_m < -1$, $x \in \Omega$ denote the piece-wise constant permittivity characterizing this problem. The total field u satisfies the following boundary value problem:

$$\begin{cases} \text{Find } u = u^{\text{in}} + u^{\text{sc}} \in H^1_{\text{loc}}(\mathbb{R}^3) \text{ such that:} \\ \nabla \cdot (\varepsilon^{-1}\nabla u) + k^2 u = 0, \quad \text{in } \mathbb{R}^3 \\ [u]_{\partial\Omega} = 0, \quad [\varepsilon^{-1}\partial_n u]_{\partial\Omega} = 0 \\ \lim_{r\to\infty} r(\partial_r - ik)u^{\text{sc}} = 0 \end{cases} \tag{1}$$

One can use T-coercivity theory to establish that (1) is well-posed and FEM converges as long as the mesh is locally symmetric at the vicinity of the interface (e.g. [1]). We solve (1) using expansions in spherical harmonics, $Y_l^m(\theta, \phi)$ with θ, ϕ, denoting the azimuthal angle, polar angle, respectively. Using the Jacobi-Anger expansion for u^{in}, we find that

$$u^{\text{sc}}(x) = \sum_{l=0}^{\infty} \left[A_l \mathbf{h}_l(kr) - C_l \mathbf{j}_l(kr)\right] Y_l^0(\theta, \phi),$$

for $x \in E$, with $C_l = i^l\sqrt{(2l+1)(4\pi)}$, and

$$u^{\text{sc}}(x) = \sum_{l=0}^{\infty} B_l \mathbf{i}_l(k_m r) Y_l^0(\theta, \phi)$$

for $x \in \Omega$. Here, $k_m = \sqrt{-\varepsilon_m}k$, and $\mathbf{h}_l$, $\mathbf{j}_l$, $\mathbf{i}_l$ are the spherical Hankel functions, the spherical Bessel functions, and modified spherical Bessel functions of the first kind and of order ℓ, respectively. Using the transmission (jump) conditions in (1), the coefficients $(A_l, B_l) \in \mathbb{C} \times \mathbb{C}$ satisfy

$$\mathcal{M}_l(k) \begin{bmatrix} A_l \\ B_l \end{bmatrix} = C_l \begin{bmatrix} \mathbf{j}_l(k) \\ -\mathbf{j}_l'(k) \end{bmatrix} \text{ with} \tag{2}$$

$$\mathcal{M}_l(k) = \begin{bmatrix} -\mathbf{h}_l^{(1)}(k) & \mathbf{i}_l(k_m) \\ \mathbf{h}_l^{(1)\prime}(k) & (-\varepsilon_m)^{-1/2}\mathbf{i}_l'(-k_m) \end{bmatrix} \tag{3}$$

The top left plot of Fig. 1 shows a plot of $\|u^{\text{sc}}\|_{L^2(D)}$ where D is a ball containing Ω as a function of k. We observe that the field peaks at some wavenumbers $(k_n)_n$ where the corresponding FEM computations (see Fig. 1, top right) show plasmonic fields. Additionally, we find that larger errors occur at those peaks.

2 Plasmonic resonances

To identify the peaks seen in Fig. 1, we find the zeros of $\det(\mathcal{M}_l(k)) = 0$ with $\mathcal{M}_l(k)$ defined in (3), in particular those which correspond to surface plasmon resonances. We find surface plasmon resonances $(k_{p,l})_l$ close to the real axis (see Fig. 1, bottom). The large peaks of $\|u^{\text{sc}}\|_{L^2(D)}$ correspond to $k = \Re(k_{p,l})$. For fixed l the plasmonic resonance k_p corresponds to plasmonic resonant mode

$$u^p(x) = \begin{cases} \frac{\mathbf{i}_l(k_{pm})}{\mathbf{h}_l(k_p)} \mathbf{h}_l(k_p r) Y_l^m(\theta, \phi), & x \in E \\ \mathbf{i}_l(k_{pm} r) Y_l^m(\theta, \phi), & x \in \Omega \end{cases} \tag{4}$$

where $k_{pm} = \sqrt{-\varepsilon_m}k_p$. The resonant mode u^p is highly oscillatory (sub-wavelength) with potential large amplitude α when excited. The FEM will fail to approximate the solution when these highly oscillatory resonant modes occur.

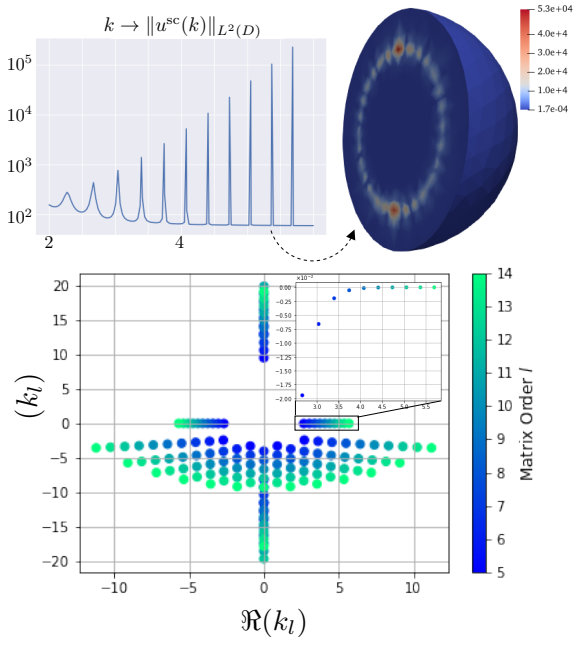

Figure 1: (Top left) L^2 norm of u^{sc} (analytic solution) with respect to k, for $\varepsilon_m = -1.1$. (Top right) Slice of the absolute error (yz-plane) using FEM (P2) and 58k DOFs on a truncated domain D (using DtN with 15 terms [3]) for k indicated by the dashed arrow: plasmonic behaviors occur. (Bottom) Associated resonances. The zoom contains the plasmonic resonances (close to the real axis, their real part match the wavenumbers obtained on the top figure).

3 Extracting plasmonic behaviors from the formulation

In order to take into account the varying scale of the resonant mode, we assume a solution u for the total field given as the sum:

$$u = u^{\text{in}} + u^{\text{reg}} + \alpha u^p, \quad \alpha \in \mathbb{C}, \tag{5}$$

where α is related to the excitation source, and $u^{\text{reg}} \in H^1_{\text{loc}}(\mathbb{R}^3)$ is smooth. The goal is to compute (u^{reg},α). Substituting (4) into (5), we derive a system for (u^{reg},α) based on weak forms of (1). We compute discrete solution $(u_N^{\text{reg}}, \alpha_h) \in \mathbb{C}^N \times \mathbb{C}$ of:

$$\begin{bmatrix} \mathbb{K}_\varepsilon + k^2\mathbb{M} + \mathbb{S} & \mathcal{U}^p \\ \mathcal{I}\mathcal{Y} & C_2 \end{bmatrix} \begin{bmatrix} u_N^{\text{reg}} \\ \alpha_h \end{bmatrix} = \begin{bmatrix} f_N \\ C_1 \end{bmatrix} \tag{6}$$

for N degrees of freedom (DOFs). Above, $\mathbb{K}_\varepsilon$ is a weighted stiffness matrix, $\mathbb{M}$ is the mass matrix, $\mathbb{S}$ is the surface matrix (obtained using the Dirichlet-to-Neumann (DtN) map on the truncated domain D), f_N is the discrete right-hand side (related to u^{in}), and $C_1, C_2 \in \mathbb{C}$ are analytic constants. Finally, $\mathcal{I}\mathcal{Y}$, $\mathcal{U}^p$ contain the coupling terms (between u^p and FEM basis function).

4 Asymptotic Quadrature

For the coupling terms in (6), one needs to accurately compute integrals such as

$$\int_D u^p \varphi_i dD, \; i \in [\![1, N]\!],$$

where φ_i is a FEM basis function. Looking at (4), high frequency behavior from the spherical harmonics combined with relatively coarse mesh (in the case of limited computational resources to approximate three-dimensional problems), or low order FEM, leads to large errors. As an alternative to refining the mesh, we make use of the asymptotic expansion of the spherical harmonics for large l. For example when $m = 0$, we have the leading behavior (see [4, p. 140]):

$$Y_l^0(0, \phi) \sim \frac{\cos\left((l + 1/2)\phi - \pi/4\right)}{\sqrt{2\pi l \sin(\phi)}}, \tag{7}$$

when $l \to \infty$. Here, we have an explicit expression for the fast oscillations in (7) which we can use to develop a product quadrature method [2]. This product quadrature method uses exact integration of polynomials multiplied by those fast oscillations to derive weights. Those weights, in turn, analytically account for the fast oscillations in u^p and relieve the FEM from having to compute them. By extending this analysis, we will develop a method for computing the coupling terms in (6) without having to resort to refining the mesh. Application to the scattering by multiple spheres (and other shapes starting with ellipsoids) and comparison with enriched elements methods will be considered in the future. Similar results could be observed for dispersive materials ($\varepsilon = \varepsilon(k)$). **Acknowledgements** This work is partially funded by the National Science Foundation Grants: DMS-2009366 and DMS-1840265.

References

[1] A.-S. Bonnet-Ben Dhia *et al.*, Mesh requirements for finite element approximation of problems with sign-changing coefficients, *Numer. Math.*, 138 (2018), pp. 801–838.

[2] L.M. Delves, J. Mohamed, Computational Methods for Integral Equations, Cambridge University Press, Cambridge, UK, 1988.

[3] J. Melenk, S. Sauter, Convergence analysis for finite element discretizations of the Helmholtz equation with Dirichlet-to-Neumann boundary conditions, *Math. Comput.* 79 (2010), pp. 1871–1914.

[4] R. Wong, Asymptotic Approximations of Integrals, Academic Press, 1989.